

UCLA

UCLA Previously Published Works

Title

Apamin induces early afterdepolarizations and torsades de pointes ventricular arrhythmia from failing rabbit ventricles exhibiting secondary rises in intracellular calcium

Permalink

<https://escholarship.org/uc/item/82v1p0zw>

Journal

Heart Rhythm, 10(10)

ISSN

1547-5271

Authors

Chang, Po-Cheng
Hsieh, Yu-Cheng
Hsueh, Chia-Hsiang
et al.

Publication Date

2013-10-01

DOI

10.1016/j.hrthm.2013.07.003

Peer reviewed

Apamin induces early afterdepolarizations and torsades de pointes ventricular arrhythmia from failing rabbit ventricles exhibiting secondary rises in intracellular calcium

Po-Cheng Chang, MD,^{*†} Yu-Cheng Hsieh, MD, FHRS, PhD,^{*} Chia-Hsiang Hsueh, PhD,^{*} James N. Weiss, MD,[‡] Shien-Fong Lin, PhD,^{*#} Peng-Sheng Chen, MD, FHRS^{*}

From the ^{*}Krannert Institute of Cardiology and the Division of Cardiology, Department of Medicine, Indiana University School of Medicine, Indianapolis, Indiana, [†]Second Section of Cardiology, Department of Medicine, Chang Gung Memorial Hospital and Chang Gung University School of Medicine, Taoyuan, Taiwan, [‡]Cardiovascular Research Laboratory, Department of Medicine (Cardiology) and Physiology, David Geffen School of Medicine, University of California, Los Angeles, California, and [#]Institute of Biomedical Engineering, National Chiao Tung University, Hsinchu, Taiwan.

BACKGROUND A secondary rise of intracellular Ca^{2+} (Ca_i) and an upregulation of apamin-sensitive K^+ current (I_{KAS}) are characteristic findings of failing ventricular myocytes. We hypothesize that apamin, a specific I_{KAS} blocker, may induce torsades de pointes (TdP) ventricular arrhythmia from failing ventricles exhibiting secondary rises of Ca_i .

OBJECTIVE To test the hypothesis that small conductance Ca^{2+} activated I_{KAS} maintains repolarization reserve and prevents ventricular arrhythmia in a rabbit model of heart failure (HF).

METHODS We performed Langendorff perfusion and optical mapping studies in 7 hearts with pacing-induced HF and in 5 normal control rabbit hearts. Atrioventricular block was created by cryoablation to allow pacing at slow rates.

RESULTS The left ventricular ejection fraction reduced from 69.1% [95% confidence interval 62.3%–76.0%] before pacing to 30.4% [26.8%–34.0%] ($N = 7$; $P < .001$) after pacing. The corrected QT interval in failing ventricles was 337 [313–360] ms at baseline and 410 [381–439] ms after applying 100 nmol/L of apamin ($P = .01$). Apamin induced early afterdepolarizations (EADs) in 6 ventricles, premature ventricular beats (PVBs) in 7 ventricles, and polymorphic ventricular tachycardia consistent with TdP in 4 ventricles. The

earliest activation site of EADs and PVBs always occurred at the site with long action potential duration and large amplitude of the secondary rises of Ca_i . Apamin induced secondary rises of Ca_i in 1 nonfailing ventricle, but no EAD or TdP were observed.

CONCLUSIONS In HF ventricles, apamin induces EADs, PVBs, and TdP from areas with secondary rises of Ca_i . I_{KAS} is important in maintaining repolarization reserve and preventing TdP in HF ventricles.

KEYWORDS Action potential duration; Apamin; Optical mapping; Potassium channels; Torsades de pointes

ABBREVIATIONS APD = action potential duration; AV = atrioventricular; Ca_i = intracellular Ca^{2+} ; EAD = early afterdepolarization; HF = heart failure; $\text{I}_{\text{Ca,L}}$ = L-type Ca^{2+} current; I_{KAS} = apamin-sensitive K^+ current; LV = left ventricular; PCL = pacing cycle length; PVB = premature ventricular beat; QTc = corrected QT; SK = small conductance Ca^{2+} activated K^+ ; TdP = torsades de pointes; V_m = membrane potential

(Heart Rhythm 2013;10:1516–1524) © 2013 Heart Rhythm Society. All rights reserved.

Introduction

Ventricular arrhythmia is a major cause of death in patients with heart failure (HF).¹ Multiple randomized clinical trials^{2–4} conducted in patients with HF documented increased

ventricular arrhythmias or mortality in patients randomized to the drug treatment arm, suggesting that HF predisposes patients to drug-induced arrhythmia. A recent study confirmed that there is enhanced sensitivity to drug-induced QT interval lengthening in patients with HF owing to left ventricular (LV) systolic dysfunction.⁵ The mechanisms by which HF increases the risk of drug-induced arrhythmia and reduces drug safety remain poorly understood. Previous studies showed that HF is associated with the downregulation of multiple K^+ currents^{6,7} but the upregulation of apamin-sensitive K^+ current (I_{KAS}) conducted through the small conductance Ca^{2+} activated K^+ (SK) channels.⁸ Drugs that block these K^+ currents may reduce repolarization reserve, prolong action potential duration (APD), and increase

This article was processed by a guest editor. This study was supported in part by National Institutes of Health (grants P01HL78931, R01HL71140, and R21HL106554), the Kawata and Laubisch Endowments (to Dr Weiss), a Medtronic-Zipes Endowment (to Dr Chen), and the Indiana University Health-Indiana University School of Medicine Strategic Research Initiative. Medtronic, St Jude Medical, and Cyberonics donated research equipment to Dr Chen's laboratory. **Address reprint requests and correspondence:** Dr Peng-Sheng Chen, Krannert Institute of Cardiology and the Division of Cardiology, Department of Medicine, Indiana University School of Medicine, 1800 N Capitol Avenue, Room E475, Indianapolis, IN 46202. E-mail address: chenpp@iu.edu.

propensity of ventricular arrhythmia. The upregulation of I_{KAS} in failing ventricles was recently reproduced by Bonilla et al⁹ in a canine model of HF. In addition to I_{KAS} upregulation, failing ventricular myocytes are known to develop a slow secondary rise of intracellular Ca^{2+} (Ca_i) that prolongs the Ca_i transient duration.¹⁰ The prolonged availability of Ca^{2+} may activate the I_{KAS} to counterbalance the downregulation of other K^+ currents, thereby maintain repolarization reserve and prevent ventricular arrhythmias in HF. If this hypothesis is correct, then blocking the I_{KAS} by apamin should reduce the repolarization reserve and promote ventricular arrhythmias in failing but not normal ventricles. This hypothesis has important implications in drug safety in HF because inadvertent blocking of I_{KAS} by food or drugs may increase the incidence of ventricular arrhythmia and sudden cardiac death. The purpose of the present study was to perform optical mapping studies in failing rabbit ventricles to test the hypotheses that apamin, a specific I_{KAS} blocker, induces early afterdepolarizations (EADs) and torsades de pointes (TdP) ventricular arrhythmias from areas with secondary rises of Ca_i in failing ventricles.

Methods

Surgical preparation

Rapid pacing protocol was conducted to induce HF in 7 New Zealand white rabbits.^{8,11} Five normal rabbits were also studied as controls. Echocardiography was performed before and after high-rate pacing. The hearts were harvested and Langendorff perfused with oxygenated 37°C Tyrode's solution that includes (in mmol/L) NaCl 125, KCl 4.5, $NaHCO_3$ 24, NaH_2PO_4 1.8, $CaCl_2$ 1.8, $MgCl_2$ 0.5, dextrose 5.5, and bovine serum albumin 100 mg/L with a pH of 7.40. Cryoablation of atrioventricular (AV) node was then performed to reduce ventricular rate. We performed simultaneous membrane potential (V_m) and Ca_i optical mapping according to methods published elsewhere.^{12,13} More detailed descriptions are included in an [Online Supplement](#).

Experimental protocol

Pseudo-electrocardiogram was monitored by using 2 electrodes placed at the left atrium and the right ventricle, respectively. A bipolar electrode was used to pace the right ventricle with an output at 2.5 times the diastolic pacing threshold. Dynamic pacing protocol¹⁴ was performed and the optical signals were mapped at different pacing cycle lengths (PCLs). We started to acquire optical mapping signal after at least 30 paced beats at the same PCL. An S1/S2/S3 short-long-short pacing protocol (S1 30 beats with S1–S1 300 ms, a long S1–S2 of 1000 or 2000 ms, and an S2–S3 starting from 300 ms and gradually shortened to the ventricular effective refractory period) was used to simulate the electrocardiographic characteristics that initiate the TdP ventricular tachycardia in humans.¹⁵ Apamin (100 nmol/L) was then added to the perfusate, and the protocol was repeated 30 minutes later. Nifedipine (2 μ mol/L) was then

added in 4 of the 7 failing rabbit hearts to determine whether it prevents the development of TdP. The same protocol was also conducted in 5 normal rabbit hearts for comparison.

Data analysis

APD_{80} was measured at the level of 80% repolarization of APD, and mean APD_{80} was calculated for all available ventricular pixels. A *secondary rise of Ca_i* is defined as the spontaneous increase in Ca_i at the downslope of the primary Ca_i released.¹⁰ Continuous variables are expressed as mean [95% confident interval]. Paired Student *t* tests were used to compare continuous variables measured at baseline and during apamin infusion. Comparison of prevalence of EAD inducibility between baseline and during apamin infusion was performed by using paired McNemar test. A $P \leq .05$ was considered statistically significant.

Results

Induction of HF

All 7 rabbits developed significant symptoms and signs of HF, including tachypnea, poor appetite, cardiomegaly, and pleural effusion. The LV ejection fraction reduced from 69.1% [62.3%–76.0%] before pacing to 30.4% [26.8%–34.0%] ($P < .001$) after pacing. LV end-diastolic diameter increased from 12.3 [11.5–13.12] to 18.1 [16.6–20.0] mm ($P < .001$) and the LV end-systolic diameter from 7.9 [7.0–8.8] to 15.7 [14.3–17.2] mm ($P < .001$). The Langendorff perfused rabbit hearts had sinus rhythm with sinus cycle length 405 [341–469] ms and normal 1:1 AV conduction before AV node cryoablation. All rabbits developed complete AV block after 1–3 attempts of cryoablation, with mean ventricular escape cycle lengths of 1757 [1217–2297] ms. After the addition of apamin, the average spontaneous ventricular escape rate did not change significantly (1757 [1176–2338] ms; $P = .99$). The sinus (atrial) cycle length did not change significantly after cryoablation (457 [366–549] ms; $P = .33$) or after adding apamin (434 [323–545] ms; $P = .62$).

Effects of apamin on QT interval and ventricular arrhythmias in failing ventricles

Apamin significantly prolonged corrected QT (QT_c) interval during spontaneous escape rhythm. The QT_c interval was 337 [313–360] ms at baseline and 410 [381–439] ms after applying 100 nmol/L of apamin ($P = .01$). [Figure 1A](#) shows an example of QT prolongation after apamin administration. [Figure 1B](#) shows the effects of apamin on QT_c intervals in all 7 hearts studied. In addition to prolonging QT_c intervals, apamin led to the development of EADs in 6 ventricles. The ventricle without EAD had a mean APD of 208 ms (at a PCL of 500 ms), which was within the range of APDs (188–261 ms at a PCL of 500 ms) in ventricles with EADs. Premature ventricular beats (PVBs) were observed in 7 ventricles and polymorphic ventricular tachycardia consistent with TdP in 4 ventricles.

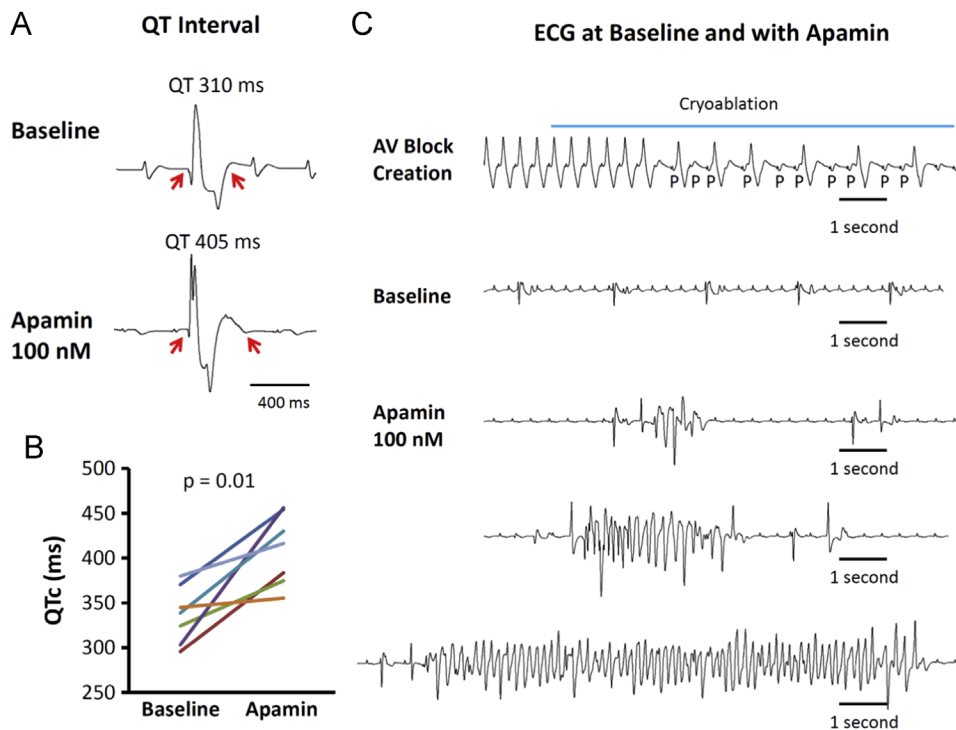


Figure 1 Apamin effect on QT interval and arrhythmias in failing hearts. **A:** Representative pseudoelectrocardiographic traces of QT interval in a failing heart with complete atrioventricular (AV) block before and after 100 nmol/L of apamin. **B:** Paired dot plot shows corrected QT (QTc) interval at baseline and in the presence of apamin (100 nmol/L). There was significant prolongation of QTc interval. **C:** Representative traces at baseline and in the presence of apamin. *Top subpanel:* Complete AV block developed during AV node cryoablation. *Middle subpanel:* No polymorphic ventricular tachycardia was recorded at baseline. *Bottom subpanels:* Several episodes of spontaneous torsades de pointes polymorphic ventricular arrhythmia developed in the presence of apamin.

Figure 1C shows the creation of AV block with cryoablation. The hearts have stable escape rhythm without arrhythmias until the administration of apamin when episodes of TdP developed spontaneously in 2 ventricles and after short-long-short pacing protocols in an additional 2 ventricles. Figure 2A shows additional examples of ventricular escape rhythm at baseline, PVBs, and an episode of TdP in the presence of apamin. Apamin significantly increased frequency of PVB in the failing ventricles (from 2.35 [−0.05 to 4.74] to 17.23 [10.65–23.8] beats/h; $P = .001$; Figure 2B, upper subpanel). The frequency of spontaneous and induced TdP was also increased from 0 [0–0] to 2.88 [0.27–5.50] episodes/h ($P = .04$; Figure 2B, lower subpanel).

Activation cycle length and the effects of apamin in failing ventricles

Apamin significantly prolonged APD₈₀ at all PCLs. The ratio of APD prolongation was larger at long PCLs than at short PCLs. Figure 3A shows representative examples of APD prolongation at different PCLs. Figure 3B shows the mean APD₈₀ without and with apamin. The color APD₈₀ maps show the heterogeneous distribution of APD₈₀ at long PCL, both before and after apamin. Figure 3C shows the ratio of Δ APD and the baseline APD. Note that the Δ APD ratio increases with the prolongation of PCL, indicating the importance of I_{KAS} in repolarization at slow heart rates.

Secondary rises of Ca_i in failing ventricles were enhanced by apamin

We observed secondary rise of Ca_i in all failing ventricles both at baseline and after apamin administration. The area occupied by secondary rises of Ca_i was 15.2% [0.25%–27.8%] of the mapped region at baseline and increased to 61.9% [50.6%–73.1%] after apamin administration ($P < .001$). Figure 4 shows that the secondary rise of Ca_i was accentuated in the presence of apamin, along with APD prolongation. Figure 4A shows a representative V_m and Ca_i traces of a failing ventricle. At long PCL (500 or 1000 ms), apamin administration enhanced secondary Ca_i rises and Ca_i transient duration. The amplitude of secondary Ca_i rises is defined as the largest deviation from a line drawn between the onset and the offset of the secondary Ca_i rise (Figure 4B). The right panels in Figure 4A show representative secondary Ca_i rises and APD₈₀ maps in the absence and presence of apamin. There were only minimal secondary Ca_i rises at baseline, but the secondary Ca_i rise became more apparent after adding apamin. The maximum secondary Ca_i rises colocalized with the areas with the longest APD (see white arrows in Figure 4A, right panels) and sites of origin of EADs (Figure 5). The secondary Ca_i rises were enhanced by apamin and may, but not always, trigger EADs and initiate an episode of TdP. We compared average (Figure 4C) and the maximum (Figure 4D) secondary Ca_i rises of all mapped pixels. The average secondary Ca_i rises of all pixels increased significantly (from 0.32% [−0.03% to 0.67%] to

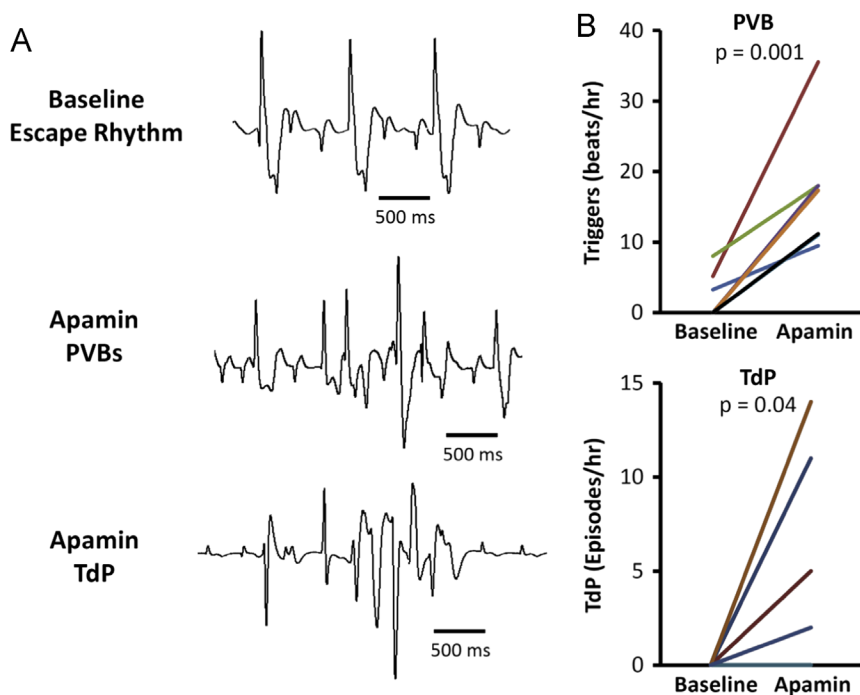


Figure 2 Comparison of premature ventricular beats (PVBs), torsades de pointes (TdP), and early afterdepolarizations at baseline and during apamin perfusion in failing hearts. **A:** Representative examples of ventricular escape rhythm at baseline (top subpanel), a PVB (middle subpanel), and an episode of TdP (bottom subpanel) in the presence of apamin. **B:** There was significant increase in PVBs and TdP during apamin (100 nmol/L) perfusion.

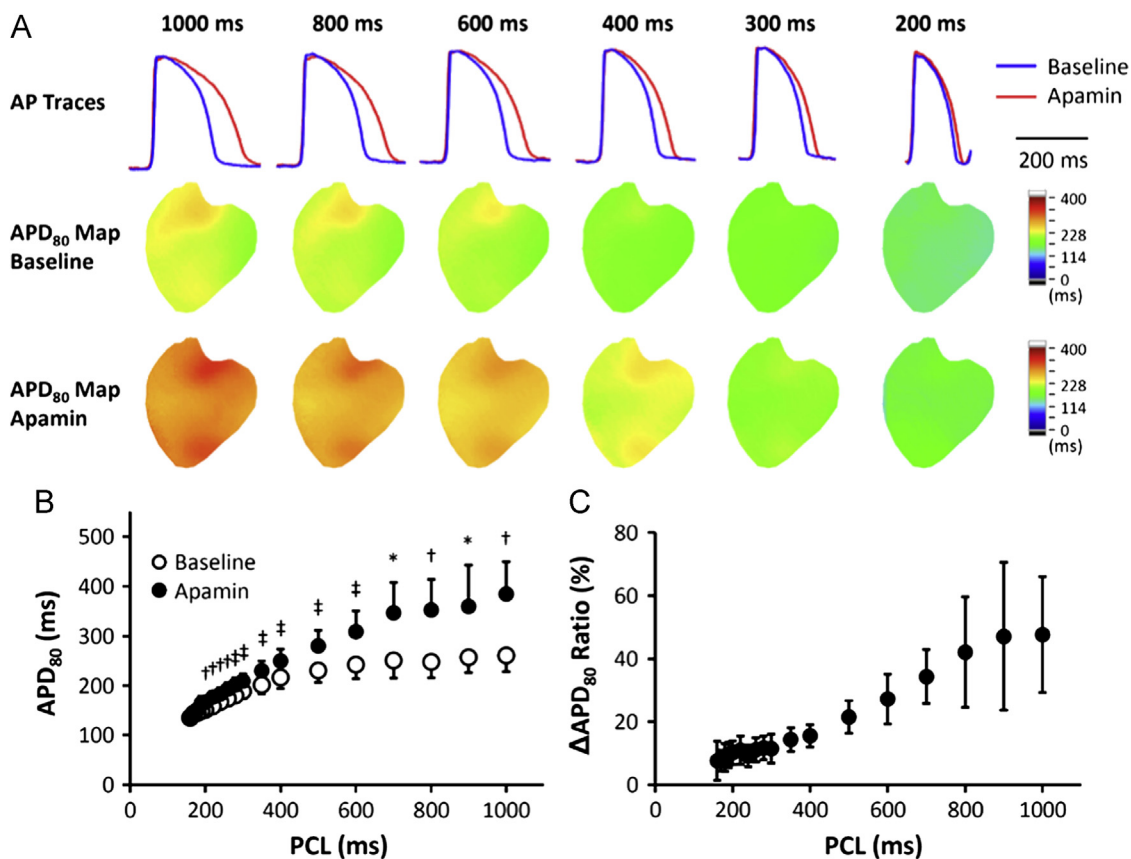


Figure 3 Apamin effect on action potential duration (APD) at different pacing cycle lengths (PCLs) in failing hearts. **A:** Representative membrane potential traces and APD₈₀ maps at baseline and in the presence of apamin (100 nmol/L). The magnitude of APD prolongation was more prominent at longer PCLs than at physiologic PCLs. **B:** Apamin significantly prolonged APD₈₀ at all PCLs, and the prolongation was more prominent at longer PCLs. **P* < .05; †*P* < .01; ‡*P* < .001. **C:** A plot of ΔAPD₈₀ ratio [(APD₈₀ after apamin – APD₈₀ at baseline)/APD₈₀ at baseline] vs PCL shows that apamin prolonged APD₈₀ by approximately 50% at a PCL of 1000 ms but only by 10% at a PCL of 200 ms.

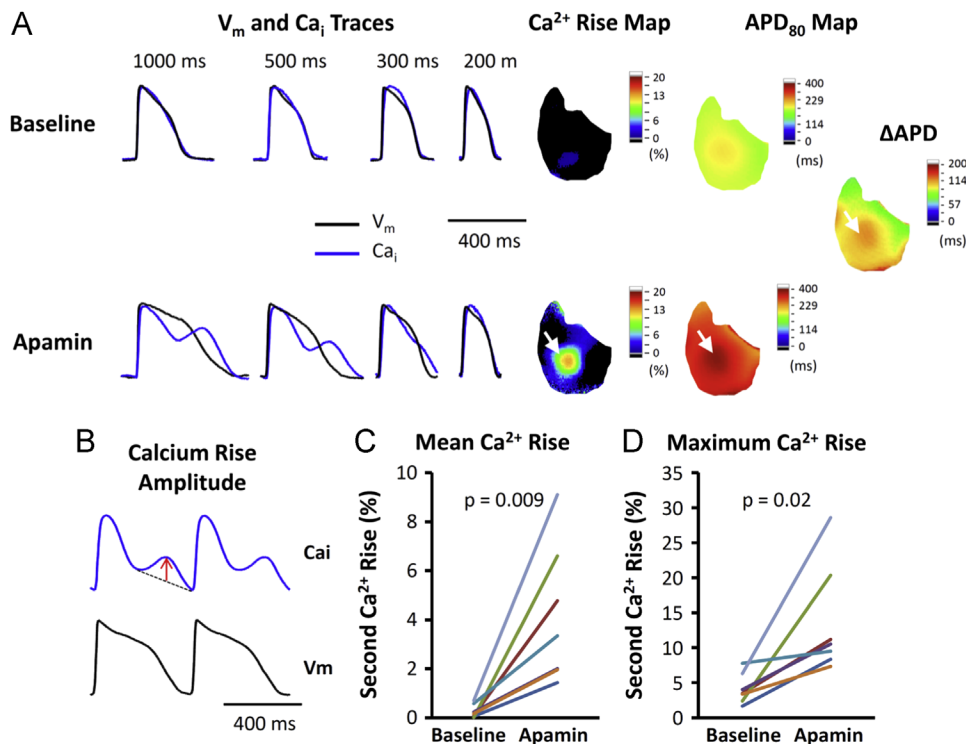


Figure 4 Secondary rises of intracellular Ca^{2+} (Ca_i) in failing ventricles. **A:** Representative membrane potential (V_m) traces, Ca_i traces, secondary rises of Ca^{2+} , and action potential duration (APD) maps at different pacing cycle lengths (PCLs) without and with apamin (100 nmol/L) perfusion. Apamin prolonged APD, along with secondary rises of Ca_i , especially at longer PCLs. The areas with the secondary rises of Ca_i colocalized with areas with the most significant APD prolongation (white arrows). The ΔAPD indicates the difference in the APD after and before apamin. **B:** The amplitude of secondary Ca_i rises is defined as the largest deviation from a line drawn between the onset and the offset of the secondary Ca_i rises, as indicated by the red arrow. **C:** Comparison of average secondary rises of Ca_i amplitude among all available ventricular pixels at baseline and in the presence of apamin (100 nmol/L) of all hearts studied. **D:** Comparison of maximal amplitude of secondary rises of Ca_i in each heart at baseline and in the presence of apamin of all hearts studied. EAD = early afterdepolarization.

3.5% [1.80% to 5.20%]; $P = .014$) in the presence of apamin. The maximum amplitude of secondary Ca_i rises was also increased (from 3.15% [1.10%–5.20%] to 13.33% [7.16%–19.50%]; $P = .03$) by apamin administration. These data indicate that apamin enhances the secondary Ca_i rises and promotes the development of EADs.

Effects of apamin on EAD and ventricular arrhythmia

Figure 5A shows the representative examples of optical mapping traces at baseline and after addition of apamin. Without apamin, HF rabbit hearts did not develop TdP arrhythmia (Figure 5A, baseline) even with short-long-short pacing. Apamin massively prolonged the APD at a PCL of 1000 ms. The corresponding Ca_i trace shows a secondary rise of Ca_i at the same pixel (Figure 5A, middle subpanel, blue trace). None of the HF rabbit hearts had EADs without apamin, and 6 (86%) hearts developed EADs or TdP in the presence of apamin ($P = .04$; Figure 5B). Figure 5C shows phase maps of the corresponding EAD beats in the spontaneous and the pacing-induced TdPs. The earliest activation sites of EAD beats colocalized with the highest secondary rises of Ca_i regions. We analyzed a total of 19 EAD episodes in 6 failing hearts (2.71 [1.53–3.90] episodes per heart). Among them, the earliest activation site of EADs and PVBs always occurred at the site with long APD and large

amplitude of the secondary rises of Ca_i . However, not all secondary rises of Ca_i resulted in EADs or PVBs. Figure 6A shows 2 different traces of spontaneous beats, one without (top subpanel) and the other with (middle subpanel) PVB. Both tracings were from the same pixel indicated by the black asterisk in Figure 6B in failing ventricles after apamin administration. Both episodes had secondary rises of Ca_i (green and red lines, respectively). When these 2 traces were superimposed on a third subpanel, it is clear that the one with PVB (red trace) had higher secondary rise of Ca_i than the one without PVB (green trace). A corresponding pseudoelectrocardiogram shows that the first QRS complex is followed by a PVB (red arrow). Figure 6D shows the phase, V_m , and Ca_i maps at the time of PVB onset. An arrow on the V_m map points to the initial propagation, which corresponds to the light blue (change in phase) in frame 617 of the phase map. Figure 6C shows the direction of propagation. The results further support an association between the amplitude of secondary Ca_i rises and the development of PVBs.

Effects of nifedipine

We tested the effects of nifedipine on apamin-enhanced secondary Ca_i rises in 4 of the 7 failing rabbit hearts. Nifedipine (2 μ mol/L) shortened APD₈₀ and reduced the slope of the primary rise of Ca_i (ie, Ca release triggered by

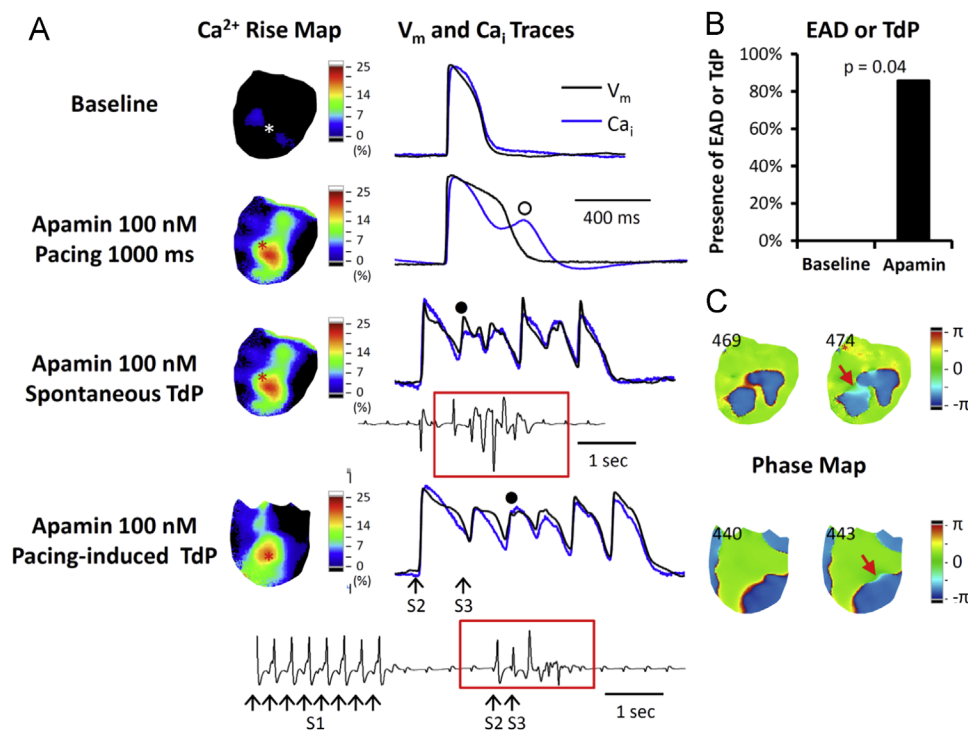


Figure 5 Relationship between secondary rises of intracellular Ca^{2+} (Ca_i) and the development of early afterdepolarization (EAD) and premature ventricular beats (PVBs) in failing hearts with atrioventricular block. **A:** The membrane potential (V_m) and Ca_i traces were taken from the site marked by an asterisk in the Ca_i rise map (map of secondary rise of Ca_i). In this pixel, the Ca_i tracing tracked the V_m tracing at baseline. Apamin prolonged action potential duration and induced secondary rise of Ca_i (unfilled circle). Subsequently, spontaneous torsades de pointes (TdP) developed from the same site with a secondary rise of Ca_i . In addition to spontaneous TdP, short-long-short (30 short S1–S1 beats and a long S1–S2 and a short S2–S3 interval) pacing protocol induced TdP in this ventricle, as shown in the bottom tracing. **B:** Apamin increased EADs and/or TdP inducibility in failing hearts. None of the hearts had EADs at baseline, and 6 of the 7 hearts developed EADs during apamin perfusion. **C:** Phase maps of the corresponding TdP beats (filled circles in panel A) in the spontaneous and the pacing-induced TdPs. Red arrows point to an area with light blue color (phase change), which is the earliest activation sites of the TdP beats. The numbers indicate frames.

depolarization). It also nearly completely eliminated the secondary rises of Ca_i in all 4 hearts (Figure 7). TdP ventricular arrhythmia and EADs were completely suppressed by nifedipine.

Effects of apamin on nonfailing rabbit ventricles

We also tested apamin effect on 5 nonfailing (control) rabbit hearts with AV block. Apamin did not prolong APD_{80} significantly at short (200 and 300 ms) PCLs (Figures 8A and 8B), but it increased APD_{80} by 25% at long PCLs (278 [227–328] ms to 346 [275–427] ms at a PCL of 1000 ms; $P = .04$). The magnitude of APD_{80} prolongation (Figure 8B) was much smaller than in the failing ventricles (Figure 3B). The ΔAPD_{80} ratio (Figure 8B) was also less than that in failing ventricles (Figure 3C). Apamin induced secondary rises of Ca_i in 1 of the 5 nonfailing ventricles at a PCL of 500 ms. No EADs or TdP were observed in that or other ventricles either before or after apamin.

Discussion

Importance of ventricular rate on the I_{KAS}

As previously reported, apamin did not significantly prolong APD at a PCL of 500 ms.^{9,16,17} However, when the PCL is lengthened to 1000 ms, even normal ventricles showed

significant APD prolongation after apamin administration. According to modeling and experimental studies,¹⁸ longer diastolic intervals are associated with a higher availability of L-type Ca^{2+} current ($I_{\text{Ca,L}}$) and longer Ca_i transient duration. The persistent trans-sarcolemmal Ca^{2+} flow through L-type Ca^{2+} channels may facilitate the SK channel activation. Therefore, blocking SK channels at long PCL prolongs APD.

Secondary rises of Ca_i

The reduced initial phase of Ca^{2+} transient, the slowed decay of Ca_i transient, and secondary rises of Ca_i are commonly observed in cardiomyocytes from failing ventricles¹⁰ but may also be present during bradycardia.¹⁹ HF reduces the initial phase of Ca^{2+} transient, which in turn reduces Ca^{2+} -induced inactivation of the $I_{\text{Ca,L}}$. As repolarization continues, the driving force for Ca^{2+} entry increases, which promotes greater Ca^{2+} entry through already opened L-type Ca^{2+} channels, leading to additional sarcoplasmic reticulum Ca^{2+} release during the latter phase of the plateau. The increased Ca^{2+} can activate sodium-calcium exchangers to prolong APD and to promote EADs. I_{KAS} in failing ventricles serves to counterbalance the APD prolonging effects of the secondary rises of Ca_i . I_{KAS} blockade, especially during bradycardia, removes this built-in counterbalance, leading to excessively prolonged APD, PVBs, and TdP arrhythmia.

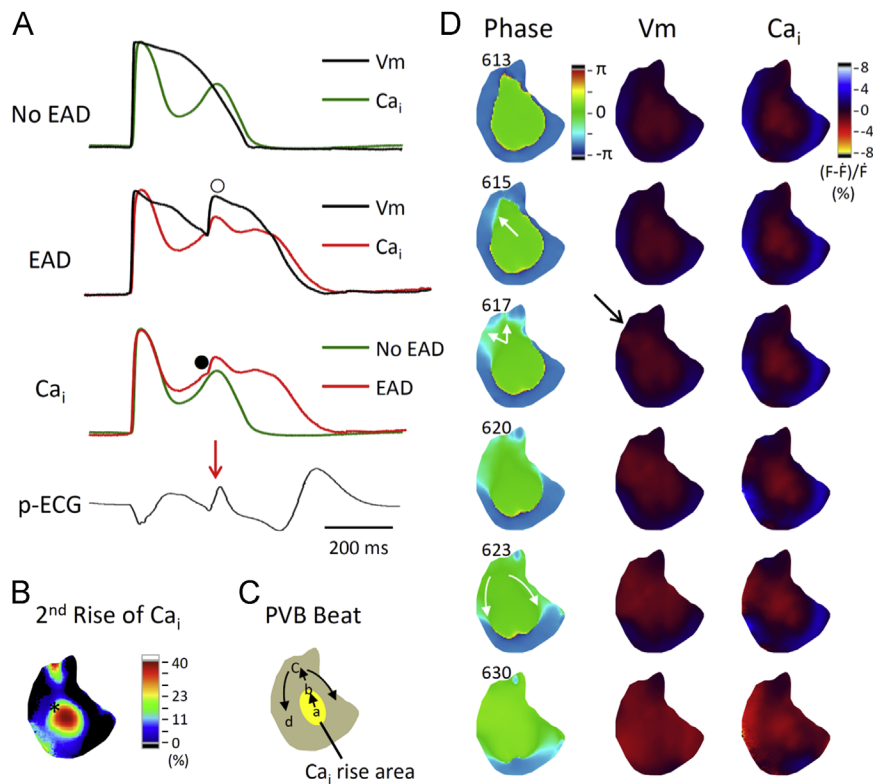


Figure 6 Secondary rises of intracellular Ca^{2+} (Ca_i) and the origin of premature ventricular beat (PVB). **A:** Membrane potential (V_m) and Ca_i traces of an automatic beat not associated with early afterdepolarization (EAD; top subpanel) and an automatic beat with EAD development (marked by unfilled circle, second subpanel) acquired from the same region (panel B, left subpanel, black asterisk). The third subpanel shows the overlaid Ca_i traces of these 2 beats. Note the red trace has higher amplitude than does the green trace. The red trace has a hump (filled circle), indicating further sarcoplasmic reticulum Ca^{2+} release induced by a propagated PVB. **B:** Secondary rise of Ca_i map of the spontaneous beat without EAD. **C:** Schematic illustration of EAD propagation. **D:** Phase, V_m , and Ca_i maps of the EAD. The EAD developed from 10 o'clock site of long action potential duration-high Ca_i area (see the light blue budding, which indicates the earliest activation of frame 615 and 617). The arrows in frame 623 indicate the direction of propagation from that early site toward the apex. pECG = pseudoelectrocardiogram.

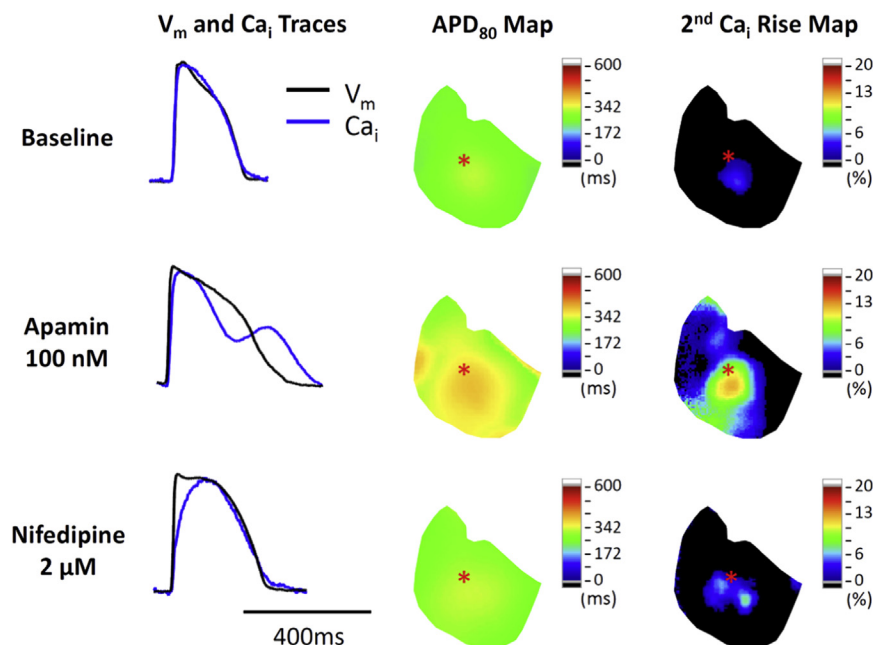


Figure 7 Representative traces and maps in a failing heart at baseline, during apamin perfusion, and after adding nifedipine. Nifedipine shortened action potential duration (APD) and ameliorated secondary rises of intracellular Ca^{2+} (Ca_i). The membrane potential (V_m) and Ca_i tracings were obtained from the site labeled by an asterisk on the APD measured at the level of 80% repolarization (APD_{80}) map and secondary Ca_i rise map. Note that the latter 2 maps show the colocalization of the secondary rises of Ca_i and the prolonged APD_{80} in the same ventricle.

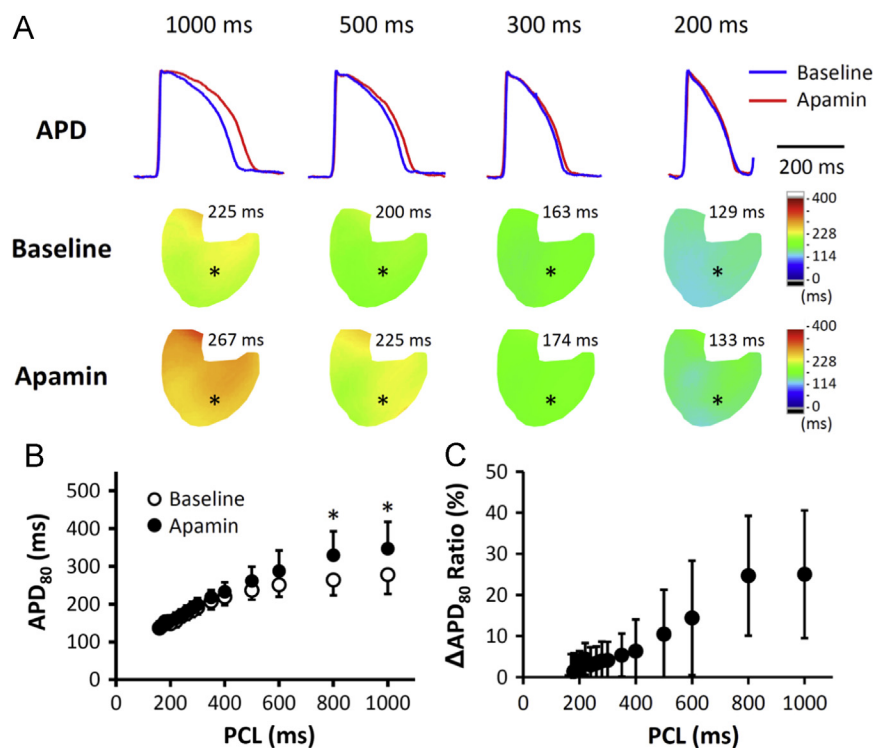


Figure 8 Apamin effect on action potential duration (APD) and secondary rises of intracellular Ca^{2+} (Ca_i) in nonfailing ventricles. **A:** Representative membrane potential (V_m) traces and APD₈₀ maps at baseline and in the presence of apamin (100 nmol/L). The results show that apamin prolonged APD at long pacing cycle lengths (PCLs), but not at physiologic PCLs. **B:** Apamin significantly prolonged APD₈₀ at PCLs 1000 and 800 ms, but not at shorter PCLs. Asterisk indicates P values of $<.05$. **C:** A plot of ΔAPD_{80} ratio [(APD₈₀ after apamin – APD₈₀ at baseline)/APD₈₀ at baseline] vs PCL.

I_{KAS} and drug safety

I_{KAS} upregulation is a mechanism by which failing ventricles maintain repolarization reserve and prevent afterdepolarizations especially in myocytes with a secondary rise of Ca_i and prolonged Ca_i transient duration. The importance of I_{KAS} in human ventricular repolarization is supported by our recent study²⁰ that showed apamin-prolonged APD in failing human ventricular cells by a mean of 11.8%. In addition to apamin, previous studies have shown that anesthetic agents such as butanol, ethanol, ketamine, lidocaine, and methohexital block recombinant SK2 channel currents.²¹ In addition, quinine, quinidine, *d*-tubocurarine, tetraethylammonium chloride, and 4-aminopyridine are I_{KAS} blockers.²² Preliminary investigation from our laboratory indicates that amiodarone is an effective I_{KAS} blocker.²³ It is possible that further investigations will discover the SK blocking action of many other drugs used in treating patients with HF. Systematic study is necessary to determine the effects of drugs or chemicals on I_{KAS} to improve the drug safety in patients with HF.

Study limitations

In addition to blocking SK currents, apamin blocks the fetal $I_{\text{Ca,L}}$.²⁴ If there is significant blockade of $I_{\text{Ca,L}}$ in rabbit ventricles, then apamin should have suppressed EADs. The fact that ventricular arrhythmias are induced by apamin suggests that either apamin is not a significant $I_{\text{Ca,L}}$ blocker or the EAD is not a mechanism of these arrhythmias. Therefore, we added nifedipine, which eliminated EADs owing to its impact on $I_{\text{Ca,L}}$. These findings further support that the EAD is

a mechanism of apamin-induced arrhythmia. Other than $I_{\text{Ca,L}}$ blockade, apamin is thought to be a highly selective blocker of SK currents.^{25–27} We propose that the results of the present study are best explained by the SK current inhibition.

Summary and clinical significance

HF is a major risk factor for drug-induced ventricular arrhythmias.²⁸ I_{KAS} , the only K current known to be upregulated in HF,⁸ may have a protective role in the failing ventricle, and efforts (intentional or secondary to off-target drug actions) to suppress this current may have proarrhythmic consequences. We showed in the present study that I_{KAS} blockade in HF ventricles results in EADs, PVBs, and TdP from areas with secondary rises of Ca_i . These findings indicate that I_{KAS} is important in maintaining repolarization reserve and preventing TdP in HF ventricles. Better understanding the drug effects on I_{KAS} may be important in the prevention of sudden death in this patient population.

Acknowledgments

We thank Nicole Courtney, Lei Lin, and Jessica Warfel for their assistance.

Appendix

Supplementary data

Supplementary data associated with this article can be found in the online version at <http://dx.doi.org/10.1016/j.hrthm.2013.07.003>.

References

1. Tomaselli GF, Zipes DP. What causes sudden death in heart failure? *Circ Res* 2004;95:754–763.
2. Echt DS, Liebson PR, Mitchell LB, et al. Mortality and morbidity in patients receiving encainide, flecainide, or placebo: the Cardiac Arrhythmia Suppression Trial. *New Engl J Med* 1991;324:781–788.
3. Waldo AL, Camm AJ, deRuyter H, et al. Effect of *d*-sotalol on mortality in patients with left ventricular dysfunction after recent and remote myocardial infarction. The SWORD Investigators. Survival With Oral *d*-Sotalol [see comments] [published erratum appears in *Lancet* 1996;348:416]. *Lancet* 1996;348:7–12.
4. Torp-Pedersen C, Moller M, Bloch-Thomsen PE, et al. Dofetilide in patients with congestive heart failure and left ventricular dysfunction. Danish Investigations of Arrhythmia and Mortality on Dofetilide Study Group. *New Engl J Med* 1999;341:857–865.
5. Tisdale JE, Overholser BR, Wroblewski HA, et al. Enhanced sensitivity to drug-induced QT interval lengthening in patients with heart failure due to left ventricular systolic dysfunction. *J Clin Pharmacol* 2012;52:1296–1305.
6. Aiba T, Tomaselli GF. Electrical remodeling in the failing heart. *Curr Opin Cardiol* 2010;25:29–36.
7. Nattel S, Maguy A, Le BS, Yeh YH. Arrhythmogenic ion-channel remodeling in the heart: heart failure, myocardial infarction, and atrial fibrillation. *Physiol Rev* 2007;87:425–456.
8. Chua SK, Chang PC, Maruyama M, et al. Small-conductance calcium-activated potassium channel and recurrent ventricular fibrillation in failing rabbit ventricles. *Circ Res* 2011;108:971–979.
9. Bonilla IM, Long VL, Vargas-Pinto P, et al. Calcium-activated potassium current modulates ventricular (but not atrial) repolarization in chronic heart failure [abstract]. *Circulation* 2012;126:A16846.
10. Piacentino V III, Weber CR, Chen X, et al. Cellular basis of abnormal calcium transients of failing human ventricular myocytes. *Circ Res* 2003;92:651–658.
11. Ogawa M, Morita N, Tang L, et al. Mechanisms of recurrent ventricular fibrillation in a rabbit model of pacing-induced heart failure. *Heart Rhythm* 2009;6:784–792.
12. Maruyama M, Joung B, Tang L, et al. Diastolic intracellular calcium-membrane voltage coupling gain and postshock arrhythmias: role of Purkinje fibers and triggered activity. *Circ Res* 2010;106:399–408.
13. Lee YS, Maruyama M, Chang PC, et al. Ryanodine receptor inhibition potentiates the activity of Na channel blockers against spontaneous calcium elevations and delayed afterdepolarizations in Langendorff-perfused rabbit ventricles. *Heart Rhythm* 2012;9:1125–1132.
14. Koller ML, Riccio ML, Gilmour RF Jr. Dynamic restitution of action potential duration during electrical alternans and ventricular fibrillation. *Am J Physiol* 1998;275:H1635–H1642.
15. Kay GN, Plumb VJ, Arciniegas JG, Henthorn RW, Waldo AL. Torsade de pointes: the long-short initiating sequence and other clinical features: observations in 32 patients. *J Am Coll Cardiol* 1983;2:806–817.
16. Nagy N, Szuts V, Horvath Z, et al. Does small-conductance calcium-activated potassium channel contribute to cardiac repolarization? *J Mol Cell Cardiol* 2009;47:656–663.
17. Xu Y, Tuteja D, Zhang Z, et al. Molecular identification and functional roles of a Ca(2+)-activated K+ channel in human and mouse hearts. *J Biol Chem* 2003;278:49085–49094.
18. Mahajan A, Shiferaw Y, Sato D, et al. A rabbit ventricular action potential model replicating cardiac dynamics at rapid heart rates. *Biophys J* 2008;94:392–410.
19. Kim JJ, Nemej J, Papp R, Strongin R, Abramson JJ, Salama G. Bradycardia alters Ca²⁺ dynamics which enhances dispersion of repolarization and arrhythmia risk. *Am J Physiol Heart Circ Physiol* 2013;304:848–860.
20. Chang P-C, Turker I, Lopshire JC, et al. Heterogeneous upregulation of apamin-sensitive potassium currents in failing human ventricles. *J Am Heart Assoc* 2013;1:e004713.
21. Drexlner JC, Jenkins A, Cao YJ, Roizen JD, Houamed KM. Patch-clamp analysis of anesthetic interactions with recombinant SK2 subtype neuronal calcium-activated potassium channels. *Anesth Analg* 2000;90:727–732.
22. Yamamoto T, Kakehata S, Yamada T, Saito T, Saito H, Akaike N. Effects of potassium channel blockers on the acetylcholine-induced currents in dissociated outer hair cells of guinea pig cochlea. *Neuroscience Lett* 1997;236:79–82.
23. Turker I, Yu C-C, Chang P, et al. Amiodarone Inhibits Apamin-Sensitive Potassium Currents. *PloS one* 2013;8:e70450.
24. Bkaily G, Sculptoreanu A, Jacques D, Economos D, Menard D. Apamin, a highly potent fetal L-type Ca²⁺ current blocker in single heart cells. *Am J Physiol* 1992;262:H463–H471.
25. Castle NA, Haylett DG, Jenkinson DH. Toxins in the characterization of potassium channels. *Trends Neurosci* 1989;12:59–65.
26. Adelman JP, Maylie J, Sah P. Small-conductance Ca(2+)-activated K(+) channels: form and function. *Annu Rev Physiol* 2012;74:245–269.
27. Ishii TM, Maylie J, Adelman JP. Determinants of apamin and *d*-tubocurarine block in SK potassium channels. *J Biol Chem* 1997;272:23195–23200.
28. Roden DM. Taking the “idio” out of “idiosyncratic”: predicting torsades de pointes. *Pacing Clin Electrophysiol* 1998;21:1029–1034.